COMPUTER SIMULATION STUDIES ON THE EFFECT OVERLAP RATIO FOR SAVONIUS TYPE VERTICAL AXIS MARINE CURRENT TURBINE

O. Bin Yaakob, K.B. Tawi and D.T. Suprayogi Sunanto*

Department of Marine Technology, Universiti Teknologi Malaysia
Postal Code 81310, UTM Skudai, Johor, Malaysia
omar@fkm.utm.my - kamarul@fkm.utm.my - x_omting@yahoo.co.id

*Corresponding Author

(Received: March 7, 2009 – Accepted in Revised Form: July 2, 2009)

Abstract The Ocean has provided a new avenue in the quest for renewable energy. One potential source of energy is marine current, which is harnessed using either vertical or horizontal axis turbines. This paper describes a particular type of vertical axis turbine which is suitable for low current velocity applications. The simulation of Savonius-type turbine, which hitherto has never been proposed for marine current energy application, is presented in this paper. A 3D computational model was built and analyzed using a Computational Fluid Dynamic analysis using proprietary software. The overlap ratio is identified as one of the important factors in Savonius turbine performance. This paper provides results of the investigation for a range of overlap ratios between 0.1 and 0.6 and it was found that the maximum torque can be obtained at overlap ratio of 0.21.

Keywords Overlap ratio, Savonius, Simulation, Computational Fluids Dynamic (CFD)

چکیده درجستجوی انرژی‌های تجدیدپذیر، اقیانوس‌ها شاه راه جدیدی را پیش روی ما می‌گذارند. جریانات دریایی منابع انرژی عظیمی هستند که می توان با گماردن توربین‌های محور افقی یا محور عمودی از پتانسیل آن‌ها بهره‌جست. در این مقاله توربین محورعمودی از نوع Savonius که در جریانات کم سرعت عملکرد خوبی داشته و تاکنون شبیه‌سازی نشده است بررسی می‌شود. با استفاده ازCFD و یک نرم افزار تخصصی، مدل محاسباتی سه‌بعدی تهیه و تحلیل شده‌است. درعملکرد توربین‌های Savonius ضریب‌هم‌پوشانی فاکتور مهمی شناخته می‌شود. در این مقاله نتایج بررسی برای ضریب هم‌پوشانی بین ۰/۱ تا ۰/٦ ارائه و بالاترین مقدار گشتاور در ضریب ۰/۲۱ بدست آمده است.

1. INTRODUCTION

The recent increase in the price of crude oil has reminded many quarters on the transient nature of fossil fuel. On the other hand, environmental issues are forcing governments to consider the incentives for development of alternative clean sources of energy. One of the potential sources of clean energy is the ocean. In this respect, a number of initiatives are being pursued by various governments, such as New Zealand [1], United Kingdom [2], Australia [3], European Union [4], the United States [5,6] and Japan [7].

There are various forms of ocean energy viz. thermal difference, tides, waves, ocean current and salinity gradient. Omar, et al [8] surveyed prospects for ocean energy in Malaysia and concluded that the most potential ocean energy source in Malaysia is in the form of marine current energy. Although capital cost is expected to be high, it has merits in low running cost, minimal environmental impact, minimal visual impact and predictability.

Currently, marine current energy is being harnessed using two types of turbines; vertical axis marine current turbines (VAMCTs) (reference [9-12]) and horizontal axis marine current turbines (HAMCTs) (reference [13-15]). Reference [16] also briefly describes and classifies some of the most common VAMCTs being currently developed. Some of the potential turbines are tabulated in Table 1.

Table 1 shows that the existing VAMCTs are mainly developed for current velocity greater than

1.1 m/s (2.45 knots). Unfortunately, Malaysian sea current velocity is much lower averaging only about 0.56 m/s or 1.1 knots [17].

Prior to this work, the authors have actually done some studies on the Chiral Blade System [18] a type of rotor for slow speed applications. Although, as shown in Figure 1, the Chiral Blade System efficiency is quite high for a slow speed flow, its complexity (with many moving parts including sophisticated gearing system) render it impractical for marine applications which normally demand for simplicity and less moving parts due to difficulty of maintenance and its exposure to corrosion. Furthermore, the system requires additional input energy to spin the blades and the rated speed of 2.0 m/s for hydro-electric generation is quite still a high as compared to typical marine current speed of 1.1 m/s in Malaysia.

TABLE 1. Various VAMCT and Specifications.

No	Vertical Axis Turbine	Current Speed [m/s]	Dimension	
			H [m]	D [m]
1	Darrieus Turbine	1.1	1.6	1.6
2	Helical Turbine	1.5	0.85	1
3	Kobold Turbine	1.8	5	6
4	Davis Turbine	2.5	1.2	1.2

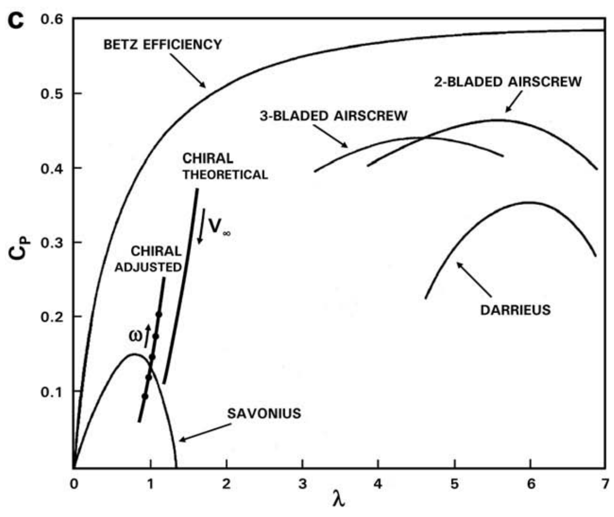

Figure 1. Comparison of Cp-λ performance curves [18].

Due to this, UTM Marine Research Group begins to explore other possibilities to harness this vast low speed ocean current energy. The exploration fortunately leads the team to the great potentials of the Savonius type turbine (usually used to extract wind energy) for the low velocity marine current applications. Being a drag-based rotor, it has the potentials to capitalize on the higher density and viscosity of seawater. The findings of this study can be found in reference [19].

For the Savonius type turbines, it is found that its performance is critically affected by 3 particular parameters. They are aspect ratio, overlap ratio and stacking configuration. The present paper describes a study on the effects of overlap ratios on the performance of the Savonius turbine in relation to its output torque.

2. MAIN PARAMETERS OF SAVONIUS TYPE ROTOR

The main parameters of a Savonius-type turbine are given in Figure 2, taken from reference [20]. Three factors are identified as affecting the performance of the Savonius-type turbine; the aspect ratio, α, how the rotors are stacked and the overlap ratio, β.

2.1. Aspect ratio The aspect ratio represents the height of rotor relative to diameter. The relation is shown by

$$\alpha = \frac{H}{D}$$

According to reference [20], conventional Savonius rotor obtained best power coefficient if α is around 4. This ratio will be applied in the present study.

2.2. Stacking Configuration The starting torque of the turbine is high but it is difficult to get a constant torque. One way of overcoming this fluctuating torque is to stack the rotors. The starting torque of double stack rotor is never negative, whatever the direction of the current.

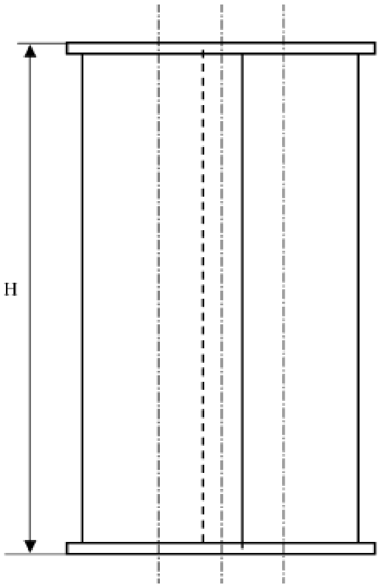

(a)

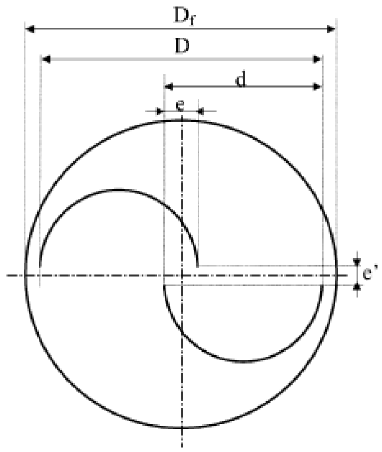

(b)

Figure 2. Schematic diagram of a single-stack Savonius, (a) Front view and (b) Top view [20].

2.3. Overlap Ratio The equation for the overlap ratio is given by

$$\beta = \frac{e}{d}$$

An experimental study described by Omar, et al [19] reported that overlap ratio is one important factor to determine the performance of the turbine. Menet [20] reported that previous experiments of Savonius-type wind turbine by a number of researchers have shown significant relationships between maximum power coefficient of turbine and the overlap ratio (β). It was stated that the maximum power coefficients were obtained at overlap ratio of between 0.20 and 0.25. It is intended in the present paper to see if similar conclusions will be obtained when Savonius-type turbine is used in marine current.

3. SIMULATION WORKS

A study was carried out on a turbine meant for producing electricity for an isolated island community. The proposed prototype dimensions are shown in Table 2.

With a scaling factor λ = 10, model dimensions and nominal current speed as well as conditions of simulation is shown in Table 3.

The simulation was run using commercial software COSMOSFloworks. This software is based on advanced Computational Fluid Dynamics (CFD) techniques and allows the user to analyze a wide range of complex problems including two and three-dimensional analyses, external and internal flows, incompressible liquid and compressible gas flows, etc. 3D modeling was made using Solidworks, and CFD was analyzed using COSMOSFloworks. The current velocity, domain boundary of model, properties of fluid and characteristic of fluid flow are the input data required.

3.1. Design Configuration of Model for Simulation In this work, the Savonius-paddle turbine model was based on the double stacking design type because; it provides smoother paddle fluctuation force to the turbine blades. Figure 3, taken from reference [19] showed comparison of a single and double stacking based on simulation using Computational Fluid Dynamic (CFD) program. The turbine with its 4 paddles is shown in Figure 4.

The turbine overlap ratios (Figure 5a) investigated in this work is between 0.1 and 0.6 at various angles of attack of the incoming current direction (Figure 5b).

3.2. Computational Domain and Initial Mesh This step determines the computational domain

TABLE 2. Main Dimensions of the Prototype.

No	Specification	Value
1	Height of Rotor, H_p	15 m
2	Diameter of Paddles, d_p	3.75 m
3	Nominal Speed, V_p	0.53 m/s–0.86 m/s

TABLE 3. Dimensions and Condition for Model Simulation.

No	Specification	Input Data
	Dimension	**Value**
1	Height of Rotor, H_m	1.5 m
2	Diameter of Paddles, d_m	0.375 m
3	Nominal Speed, V_m	0.169 m/s
	Condition	**Description**
4	Analysis Type	External Flow
5	Fluid	Water (ρ = 1000 kg/m^3)

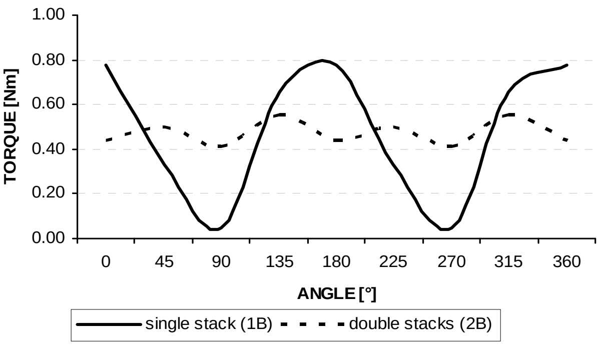

Figure 3. Smoothing of torque by double-stacking [16].

simulation and its boundary conditions are based on the XYZ axes. The computational domains of the Savonius turbines is divided into 2 parts and are based on the double stacking rotor type i.e. the upper rotor and lower rotor. Table 4 shows the input data for their computational domain.

Figure 6 shows an example of the initial mesh for one of the configuration (β=0.21) and the result

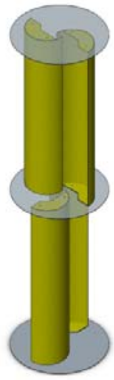

Figure 4. Savonius models for simulation, Where Paddle 1 [F_1] (b) Paddle 2 [F_2] (c) Paddle 3 [F_3] (d) Paddle 4 [F_4].

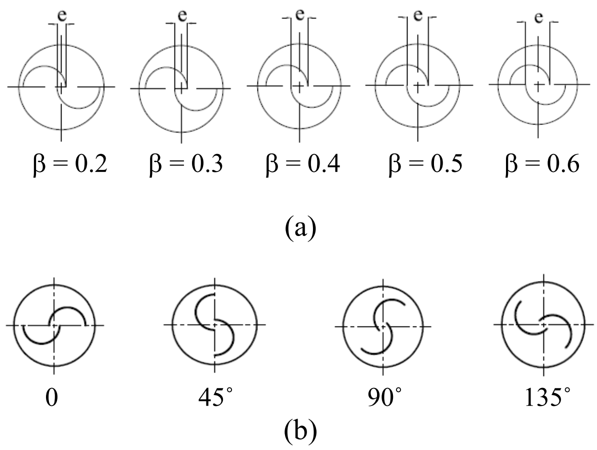

Figure 5. Rotor configuration (a) Overlap ratio configuration, (b) Angle of attack.

TABLE 4. Input Data for Computational Domain of Simulation using COSMOS Floworks.

N	Input Data	Value [m]
1	X_{min}	-1.5
2	X_{max}	1.5
3	Y_{min}	-0.75
4	Y_{max}	0
5	Z_{min}	-1.5
6	Z_{max}	1.5

of all the forces acting on the paddle are summarized in Table 5.

Table 5 shows the simulation results using COSMOSFloworks where, F_1 and F_2 are forces on paddle 1 and 2 respectively, F_3 and F_4 are forces on paddle 3 and 4 respectively. The following section describes briefly, the calculation process to obtain the required torque on the turbine, paddle from the inputs forces determined from this section.

3.3. Simulation Results Cosmos Floworks provides among other, pressure variation on the paddle. Figure 7 shows pressure contour of simulation condition at 0˚, 45˚, 90˚, and 135˚.

The simulation also yields forces on the paddles, from which the torque of turbine can be calculated. The forces on every paddle for every angle were calculated to provide the resultant force, based on Figure 8.

The torques is calculated using the following formula:

$$T_\theta = \sum_{n=1}^{n} F_n . d$$

Figure 8 shows the direction and distance of force from the center of the turbine-shaft. The torque at

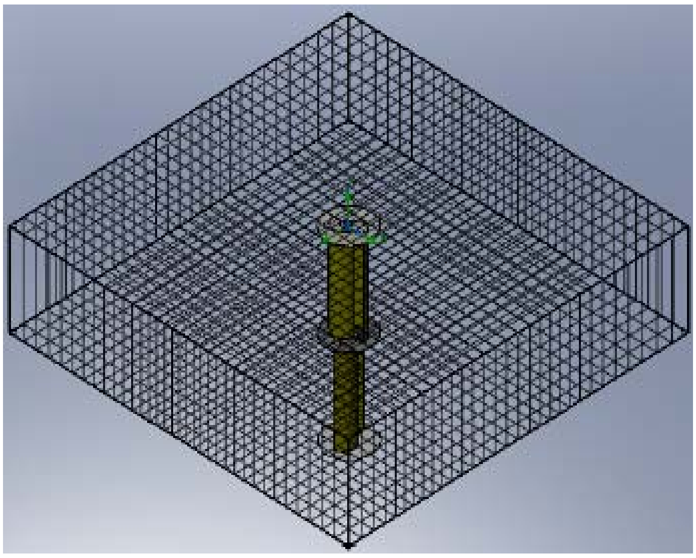

Figure 6. Meshing of the model.

TABLE 5. Example of Results From the Simulation using COSMOS Floworks.

Description	Unit	Value	Averaged Value	Minimum Value	Maximum Value	Progress [%]
Paddle 1 (F_1)	[N]	2.58	2.6	2.58	2.61	100
Paddle 2 (F_2)	[N]	0.88	0.88	0.88	0.89	100
Paddle 3 (F_3)	[N]	0.7	0.7	0.7	0.7	100
Paddle 4 (F_4)	[N]	0.5	0.5	0.5	0.5	100

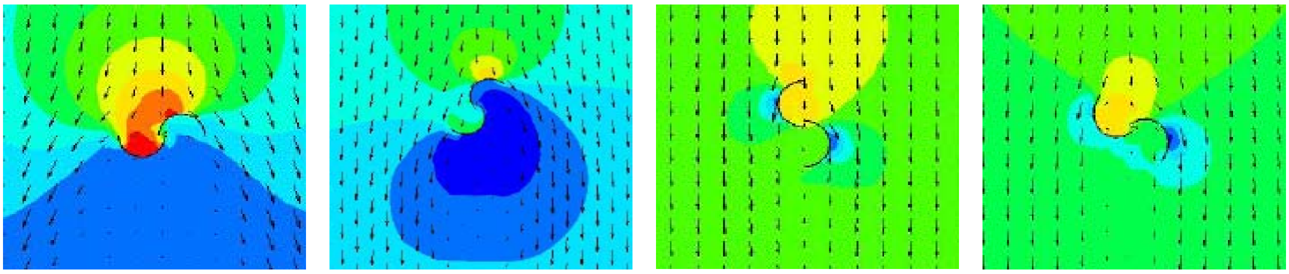

0 | 45° | 90° | 135°

Figure 7. Contour of pressure on the turbine at various angles of attack.

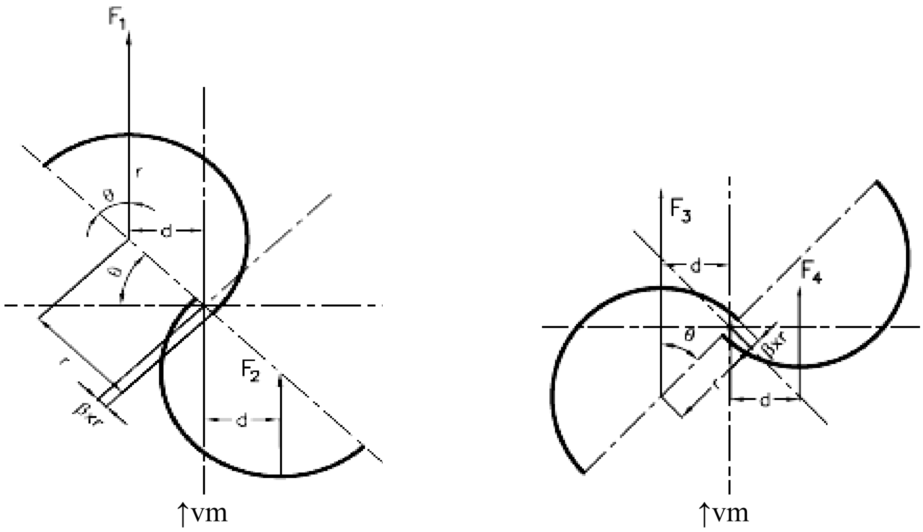

(a) (b)

Figure 8. Force direction on the paddle turbine for θ = 45°, (a). Upper rotor and (b). Lower rotor.

every angle of attack (T_θ) can be determined by the following formula:

$$T_\theta = \sum_{n=1}^{n} F_n.d$$

$$T_\theta = F_1.(r-\beta.r).\cos\theta - F_2.(r-\beta.r).\cos\theta +$$
$$F_3.(r-\beta.r).\sin\theta - F_4.(r-\beta.r).\sin\theta$$

$$T_\theta = (F_1 - F_2).(1-\beta).r.\cos\theta + (F_3 - F_4).(1-\beta).r.\sin\theta$$

The average torque (T_m) is calculated as follows:

$$T_m = \frac{\sum_{\theta=0}^{\theta} T_\theta}{i}$$

Results of the simulation are given in Table 6 and plotted in Figures 9 and 10.

4. DISCUSSIONS

Data of the torque variations with angle of attack β for overlap ratios of 0.1 to 0.15 (from Table 6) are shown in Figure 9. The sinusoidal fluctuations of the torque for the four paddles applications are as expected. Plots for other overlap ratios (β=0.19-0.60) show similar sinusoidal characteristics (not shown) however, their values are different from each other. The average torque obtained for the various overlap ratios are shown in Figure 10.

TABLE 6. Forces and Torque on Turbine Paddles with Vm = 0.169 m/s.

No	β Ratio	θ [degree]	F_1 [N]	F_2 [N]	F_3 [N]	F_4 [N]	Torque (T_θ) [Nm]	Average Torque (T_m) [Nm]
Vm = 0.169 m/s								
1	0.10	0	2.76	1.40	0.51	0.48	0.11	0.0853
		45	1.44	1.78	0.44	1.73	0.06	
		90	0.48	0.51	1.40	2.75	0.11	
		135	0.44	1.72	1.81	1.47	0.06	
2	0.11	0	2.74	1.37	0.52	0.51	0.11	0.0920
		45	1.27	1.24	0.44	1.72	0.08	
		90	0.52	0.51	1.36	2.75	0.12	
		135	0.43	1.73	1.75	1.48	0.06	
3	0.12	0	2.76	1.34	0.54	0.51	0.12	0.0915
		45	1.49	1.71	0.43	1.74	0.06	
		90	0.53	0.52	1.34	2.74	0.12	
		135	0.35	1.74	1.71	1.52	0.07	
4	0.125	0	2.75	1.31	0.53	0.52	0.12	0.0942
		45	1.54	1.65	0.41	1.76	0.07	
		90	0.54	0.53	1.31	2.74	0.12	
		135	0.41	1.76	1.65	1.54	0.07	
5	0.13	0	2.73	1.27	0.54	0.53	0.12	0.0975
		45	1.56	1.62	0.38	1.79	0.08	
		90	0.53	0.53	1.26	2.73	0.12	
		135	0.39	1.80	1.63	1.57	0.08	
6	0.15	0	2.71	1.22	0.56	0.51	0.12	0.1057
		45	1.71	1.50	0.41	1.84	0.09	
		90	0.57	0.51	1.22	2.71	0.12	
		135	0.40	1.84	1.50	1.71	0.09	
7	0.19	0	2.73	1.12	0.44	0.60	0.124	0.1228
		45	1.98	1.16	0.42	1.89	0.124	
		90	0.44	0.60	1.12	2.68	0.120	
		135	0.42	1.88	1.18	1.99	0.123	
8	0.20	0	2.67	1.05	0.37	0.68	0.12	0.1281
		45	2.12	1.02	0.41	1.85	0.13	
		90	0.37	0.68	1.05	2.67	0.12	
		135	0.41	1.85	1.02	2.12	0.13	
9	0.21	0	2.58	0.88	0.70	0.50	0.126	0.1362
		45	2.10	0.83	0.32	1.84	0.146	
		90	0.70	0.50	0.88	2.59	0.127	
		135	0.32	1.84	0.83	2.10	0.146	
10	0.25	0	2.55	0.75	0.70	0.48	0.13	0.1320
		45	2.06	0.80	0.34	1.83	0.14	
		90	0.71	0.48	0.75	2.55	0.13	
		135	0.33	1.83	0.82	2.10	0.14	

11	0.30	0	2.58	0.77	0.68	0.46	0.12	0.1266
		45	1.79	0.67	0.14	1.93	0.13	
		90	0.68	0.46	0.77	2.58	0.12	
		135	0.14	1.93	0.70	1.80	0.13	
12	0.35	0	2.46	0.70	0.51	0.50	0.11	0.1162
		45	1.67	0.68	-0.02	1.91	0.13	
		90	0.51	0.50	0.70	2.45	0.11	
		135	-0.02	1.90	0.68	1.67	0.13	
13	0.40	0	2.48	0.60	0.54	0.42	0.11	0.1079
		45	1.61	0.73	-0.06	1.84	0.11	
		90	0.54	0.43	0.60	2.46	0.10	
		135	-0.05	1.85	0.73	1.61	0.11	
14	0.45	0	2.47	0.52	0.58	0.42	0.10	0.0925
		45	1.43	0.96	-0.12	1.79	0.09	
		90	0.56	0.42	0.52	2.39	0.10	
		135	-0.12	1.80	0.96	1.42	0.09	
15	0.50	0	2.44	0.42	0.64	0.46	0.10	0.0841
		45	1.32	0.99	-0.13	1.69	0.07	
		90	0.65	0.46	0.42	2.54	0.10	
		135	-0.13	1.68	0.99	1.32	0.07	
16	0.55	0	2.63	0.88	0.64	0.75	0.07	0.0575
		45	0.91	1.20	0.28	1.48	0.03	
		90	0.63	0.78	0.40	2.63	0.09	
		135	0.42	1.58	1.13	1.14	0.03	
17	0.60	0	2.66	0.46	0.45	0.54	0.08	0.0669
		45	1.20	0.94	-0.12	1.44	0.05	
		90	0.45	0.53	0.46	2.66	0.08	
		135	-0.12	1.44	0.94	1.20	0.05	

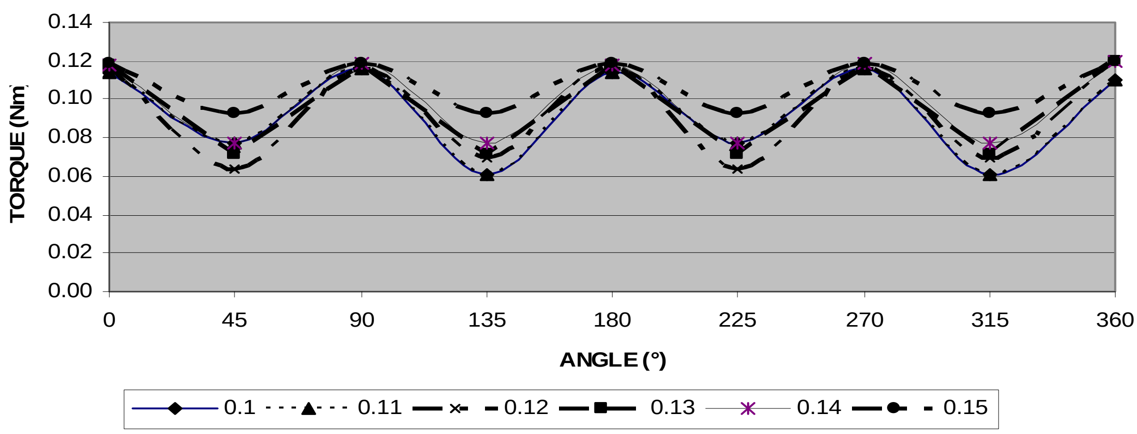

Figure 9. Torque variation with angle of attack for overlap ratios range of 0.1–0.15 with Vm = 0.169 m/s.

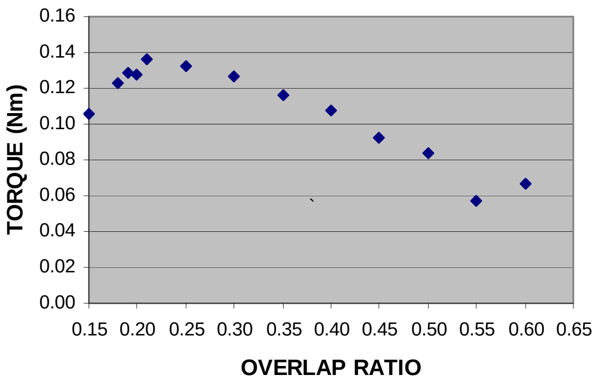

Figure 10. Torque variation for different overlap ratios.

As mentioned earlier, Menet [20] has indicated that previous studies on Savonius wind-turbines showed that maximum power coefficient occurs at β = 0.2-0.25. Gupta [21] also concluded that overlap ratios between 0.20 and 0.25 provides maximum power coefficients. This studies seems to confirm these findings for the Savonius marine current turbine as shown in Figure 10 where, the peak torque takes place at about β = 0.21.

5. CONCLUSIONS

This simulation study shows that vertical axis Savonius turbine has good potentials for low marine current velocity application. The most recommended overlap ratio for this type of turbine is β = 0.21. This is similar to the results of studies on Savonius turbine for wind turbine applications. This study also shows that the actual torque behaviour of this turbine is sinusoidal in nature and their values are always positive, showing this kind of turbine is suitable for mechanical application.

6. NOMENCLATURE

α	Aspect ratio
β	Overlap ratio
λ	Conversion factor
ρ	Density [kg/m^3]
ω	Angular velocity [rad/s]
d	Diameter of the cylinder (paddle) in the rotor/distance for torque calculation [m]
D	Diameter of rotor [m]
e	Gap between two paddles :main overlap [m]
e’	Gap between two paddles :second overlap
F	Force of turbine [N]
g	Coefficient of gravity [m/s^2]
H	Height of turbine [m]
i	Number of angle of attack
n	Number of force on the rotor
N	Rotation velocity [rpm]
P	Power [watts]
r	Radius [m]
T	Torque of model [Nm]
V	Current velocity [m/s]

Subscript

θ	Angle of attack
m	Model
p	Prototype
r	Rotor
s	Shaft

7. REFERENCES

1. Zealand Energy Efficiency and Conservation Authority, “Marine Energy: Summary of Current Developments And Outlook New Zealand”, (May 2006).
2. Boud, R., UK Department of Trade and Industry, “Wave and Marine Current Energy: Status and Research and Development Priorities”, DTI Report Number Fes-R-132, (2003).
3. Hobart, E.St., Sustainable Energy Development Office, “Study of Tidal Energy Technologies For Derby Government of Western Australia”, Report No. Wa-107384-Cr-01, (December 2001).
4. Lemonis, G., Centre For Renewable Energy Sources (CRES), “Wave Energy Utilization in Europe, Current Status and Perspectives”, European Commission Directorate-General for Research, (2002).
5. U.S. Department of the Interior, “Technology White Paper on Wave Energy Potential on the U.S. Outer Continental Shelf”, Minerals Management Service Renewable Energy and Alternate Use Program, Washington, U.S.A., (May 2006).
6. U.S. Department of the Interior, “Technology White Paper on Ocean Current Energy Potential on the U.S. Outer Continental Shelf”, Minerals Management Service Renewable Energy and Alternate Use Program, Washington, U.S.A., (May 2006).
7. Japan Marine Science and Technology Centre,

"Research and Development Technology on Wave Energy Utilization", JAMSTEC, (2004).
8. Yaakob, O., Ariff, M.A.R., Afifi, M.A.A, "Prospects for Ocean Energy in Malaysia", ***International Conference on Energy and the Environment***, Kuala Lumpur, Malaysia, (August 2006), 28-30.
9. Kiho, S, Shiono, M. and Suzuki, K., "The Power Generation from Tidal Currents by Darrieus Turbine", ***Renewable Energy***, Vol. 9, (December 1996), 1242-1245.
10. Gorlov, A.M., "Harnessing Power from Ocean Currents and Tides", ***Sea Technology***, (July 2004), 40-43.
11. Powertech Lab Inc, "Ocean energy: Global Technology Development", IEA-OES Document T0104, Canada, (2009), 63.
12. Eriksson, M.H., Moroso, A., Fiorentino, A., "The Vertical Axis Kobold Turbine in the Strait of Messina-a Case Study of a full Scale Marine Current Prototype", Ponte Di Archimede S.p.A., Italy, (2005).
13. Davis, B.V., "Low Head Tidal Power-a Major Source of Energy From the Worlds Oceans", ***Energy Conversion Engineering Conference***, (August 2007), 1982-1989.
14. Myers, L. and Bahaj, A.S., "Simulated Electrical Power Potential Harnessed by Marine Current Turbine Arrays in the Alderney Race", ***Renewable Energy***, Vol. 3, (2005), 1713-1731.
15. Fraenkel, P.L., "Marine Current Turbines: An Emerging Technology", Scottish Hydraulics Study Group Seminar, Glasgow, Lanarkshire, U.K., Vol. 19, (March 2004).
16. Batten, W.M.J., Bahaj, A.S., Molland, A.F. and Chaplin, J.R., "Experimentally Validated Numerical Method for the Hydrodynamic Design of Horizontal Axis Tidal Turbines", ***Ocean Engineering***, Vol. 34, (2007), 1013–1029.
17. Yaakob, O., Abdul Ghani, M.P., Tawi, K.B., Suprayogi, D.T., Aziz, A. and Bin Jaafar, Kh.E., "Development of Ocean Wave and Current Energy Device", ***Proceedings Seventh UMT International Symposium on Sustainability Science and Management (UMTAS)***, Kuala Terengganu, Malaysia, (June 2008), 519-530.
18. Royal Malaysian Navy, "Tide Tables Malaysia 2005", The Hydrographic Department Royal Navy Malaysia, Kuala Lumpur, Malaysia, (2005).
19. Giudice, F. and La Rosa, G., "Design, prototyping and experimental testing of a chiral blade system for Hydroelectric Microgeneration", Mechanism and Machine Theory, Vol. 44, (2009), 1463-1484.
20. Yaakob, O., Tawi, K.B. and Suprayogi, D.T., "Development of Vertical Axis Marine Current Turbine Rotor", ***International Conference Marine Renewable Energy***, U.K., (November 2008), 77-83.
21. Menet, J.-L., "A double-Step Savonius Rotor for Local Production of Electricity: A Design Study", ***Renewable Energy***, Vol. 29, (2004), 1843-1862.
22. Gupta, R., Biswas, A., Sharma, K.K., "Comparative Study of Three-Bucket Savonius Rotor with a Combined Three-Bucket Savonius-Three Bladed Darrieus Rotor", ***Renewable Energy***, Vol 33, (2008), 1974-1981.